The Astronomical Journal, 127:728–735, 2004 February

NEAR-INFRARED COLORS OF SUBMILLIMETER-SELECTED GALAXIES

D. T. Frayer,[1] N. A. Reddy,[2] L. Armus,[1] A. W. Blain,[2] N. Z. Scoville,[2] and Ian Smail[3]
Received 2003 August 11; accepted 2003 October 22

ABSTRACT

We report on deep near-infrared (NIR) observations of submillimeter-selected galaxies (SMGs) with the Near-Infrared Camera (NIRC) on the Keck I telescope. We have identified *K*-band candidate counterparts for 12 out of 15 sources in the SCUBA Cluster Lens Survey. Three SMGs remain nondetections with *K*-band limits of $K > 23$ mag, corrected for lensing. Compensating for lensing, we find a median magnitude of $K = 22 \pm 1$ mag for the SMG population, but the range of NIR flux densities spans more than a factor of 400. For SMGs with confirmed counterparts based on accurate positions from radio, CO, and/or millimeter continuum interferometric observations, the median NIR color is $J-K = 2.6 \pm 0.6$ mag. The NIR-bright SMGs ($K < 19$ mag) have colors of $J-K \simeq 2$ mag, while the faint SMGs tend to be extremely red in the NIR ($J-K > 3$ mag). We argue that a color selection criterion of $J-K \gtrsim 3$ mag can be used to help identify counterparts of SMGs that are undetected at optical and radio wavelengths. The number density of sources with $J-K > 3$ mag is 5 arcmin^{-2} at $K < 22.5$ mag, greater than that of SMGs with $S(850\ \mu\mathrm{m}) > 2$ mJy. It is not clear if the excess represents less luminous infrared-bright galaxies with $S(850\ \mu\mathrm{m}) \lesssim 2$ mJy, or if the faint extremely red NIR galaxies represent a different population of sources that could be spatially related to the SMGs.

Key words: galaxies: active — galaxies: evolution — galaxies: formation — galaxies: starburst

1. INTRODUCTION

The identification of the optical counterparts of the high-redshift population of submillimeter galaxies (SMGs; Smail, Ivison, & Blain 1997; Hughes et al. 1998; Barger, Cowie, & Sanders 1999a; Eales et al. 1999, 2000; Cowie, Barger, & Kneib 2002; Chapman et al. 2002a; Scott et al. 2002; Smail et al. 2002; Blain et al. 2002; Webb et al. 2003) is challenging because of the large beam size of the 850 μm detections and the general faintness of their rest-frame ultraviolet continuum emission (e.g., Smail et al. 2002). The most successful technique has been to use accurate radio positions to identify candidate counterparts (Smail et al. 2000; Barger, Cowie, & Richards 2000; Ivison et al. 2002; Chapman et al. 2001, 2003a). Unfortunately, current radio observations only detect about 50%–70% of the population (Smail et al. 2000; Chapman et al. 2003a), of which most are at $z \sim 2$–3 (Chapman et al. 2003b). For sources that lack radio detections, we are forced to alternative techniques for identification of the counterparts. For example, Smail et al. (1999) identified two candidate counterparts based on their being extremely red objects (EROs; $R-K > 6$ mag). EROs have been shown to contribute statistically to the 850 μm background (Wehner, Barger, & Kneib 2002), suggesting a natural connection between dusty SMGs and galaxies with extremely red colors. However, the identification of ERO counterparts based on their $R-K$ colors is limited to only the brightest examples, since most SMGs have $K > 21$ mag and typical *R*-band limits are $R < 27$ mag. A similar strategy can be applied using near-infrared (NIR) colors. Recent deep NIR surveys have shown the usefulness of the $J-K$ colors for the identification of extremely red galaxies (e.g., Totani et al. 2001b; Franx et al. 2003). By using $J-K$ colors we can identify extremely red galaxies in the SMG fields at fainter depths than currently achievable by using $R-K$.

In this paper we discuss deep NIR observations of SMGs in the SCUBA Cluster Lens Survey (Smail et al. 1997, 2002). This survey represents sensitive submillimeter mapping of seven gravitational-lensing clusters, which uncovered 15 background SMGs. The advantage of this sample is that the amplification of the background SMGs by the clusters allows for deeper source-frame observations. Previous *K*-band observations of the fields only reached depths of $K \sim 21$ mag (Smail et al. 2002), which was not sufficient to identify about half of the SMGs. The goals of these NIR observations are straightforward. In fields with no clear *K*-band counterparts, we observed much deeper in *K*-band to search for very faint sources (e.g., Frayer et al. 2000). In fields with candidate *K*-band counterparts, we observed in both *J*- and *K*-band to measure the $J-K$ colors of the population and to attempt to identify the most likely counterparts based on extremely red $J-K$ colors.

A cosmology of $H_0 = 70$ km s^{-1} Mpc^{-1}, $\Omega_M = 0.3$, and $\Omega_\Lambda = 0.7$ is assumed throughout this paper.

2. OBSERVATIONS AND DATA REDUCTION

We observed the SCUBA Lens Cluster SMGs using the Near Infrared Camera (NIRC) on the Keck I[4] telescope during seven nights between UT 1999 October and 2002 March. The NIRC instrument uses a 256×256 InSb detector with a pixel scale of 0.″15 (Matthews & Soifer 1994). We observed using the standard *J*-band (1.2 μm) and *K* band (2.2 μm) filters. Exposures of 10 s $\times$ 6 co-adds were taken in the *K* band, while exposures of 20 s $\times$ 3 co-adds were taken in the *J* band. To provide uniform coverage across the image, a random dithered pattern was used with 10″–15″ offsets between adjacent

[1] *Spitzer* Science Center, MS 220-06, California Institute of Technology, Pasadena, CA 91125.
[2] Department of Astronomy, MS 105-24, California Institute of Technology, Pasadena, CA 91125.
[3] Institute for Computational Cosmology, University of Durham, South

[4] The W. M. Keck Observatory is operated as a scientific partnership among the California Institute of Technology, the University of California, and NASA. The Keck Observatory was made possible by the generous financial support of the W. M. Keck Foundation.

exposures. The seeing during the nights varied from about 0.″4 to 1.″0 (FWHM). Approximately 15% of the data with relatively poor seeing (>0.″8) or seriously affected by internal reflections of moonlight were rejected. Residuals due to the Moon partially affect the sensitivity of the *J*-band data of SMM J00265+1710 and the *K*-band data of SMM J00267+1709. Table 1 summarizes the observing runs and provides the effective integration time on each SMG field after data editing.

We used the IRAF[5] NIRCtools package (D. Thompson 2000, private communication) to reduce the data. Sets of dark frames from each night were subtracted from each exposure to remove the dark current, as well as the bias level. The dark-subtracted exposures were divided by a normalized sky flat. Frames were sky-subtracted using temporally adjacent images to yield reduced exposures. The individual exposures were aligned to the nearest pixel using common objects in the frames. The data were placed on the Vega-magnitude scale from observations of a set of NIR standard stars (Persson et al. 1998) taken at a range of air masses to correct for extinction. Based on the dispersion of zero points determined throughout the runs, the uncertainty of the derived magnitude scale is about 0.05 mag for large apertures.

Data from multiple nights were combined with weights proportional to their integration times. For source identification and photometry, we used the SExtractor program (Bertin & Arnouts 1996). The reduced *J*- and *K*-band maps were combined to produce deeper NIR images for source detection. These combined images were used as the reference images to define the aperture centers for photometric measurements on the individual *J*- and *K*-band images. Weight maps proportional to the inverse of the local variance were used to yield representative errors. The images were registered to the Automatic Plate Measuring (APM) coordinate system using optical data of the fields from Smail et al. (2002). For the case of SMM J04433+0210 (N4), we adopted the updated astrometric solution from Neri et al. (2003).

[5] IRAF is distributed by the National Optical Astronomy Observatory, which is operated by the Association of Universities for Research in Astronomy, Inc., under cooperative agreement with the National Science Foundation.

3. RESULTS

Figure 1 shows the *J*- and *K*-band images of the SMG fields. The extent of the images matches the FWHM beam of the Submillimeter Common User Bolometric Array (SCUBA) instrument at 850 μm. The images are centered on the submillimeter positions listed in Table 1, which are accurate to about 3″ for the brightest submillimeter sources. For all but three sources, we adopted the submillimeter positions given by Smail et al. (2002). In the case of SMM J22471−0206, the peak position of the submillimeter emission was used. This is offset by about 4″ northwest from the position tabulated by Smail et al. (2002), and the uncertainty in the position of SMM J22471−0206 may result from blending with a fainter submillimeter source. For SMM J21536+1742 the position from the subsequent deeper observations from Cowie et al. (2002) was used. We also adopted an average central position for SMM J02400-0134 based on the Smail et al. (2002) position and the position of Cowie et al.'s (2002) source 2. Galaxies previously identified are labeled with their name ID given by Smail et al. (2002). New candidate SMG counterparts are designated with an "A," and additional extremely red NIR ($J-K > 3$ mag) sources in the fields are designated with a "B."

3.1. *Photometry Results*

Table 2 shows the results of aperture measurements for the confirmed and candidate counterparts of the SMGs. The confirmed SMG counterparts are based on accurate positions from CO, millimeter continuum, and/or radio interferometric observations (see references in Table 2). The candidate counterparts are discussed in § 3.2. For the majority of the sources, which are small, a 14 pixel diameter aperture (2.″05) was used, while larger apertures were used as appropriate for extended sources. Aperture corrections, as a function of aperture size, were calculated using the observations of standard

TABLE 1
NIRC Observations

Source	S(850 μm) (mJy)	Submillimeter α (J2000.0)	Submillimeter δ (J2000.0)	K Band (minutes)	J Band (minutes)
SMM J02399−0136	23.0	02 39 51.9	−01 35 59	13	13
SMM J00266+1708	18.6	00 26 34.1	+17 08 32	144	62
SMM J09429+4658	17.2	09 42 54.7	+46 58 44	32	121
SMM J14009+0252	14.5	14 00 57.7	+02 52 50	70	62
SMM J14011+0252	12.3	14 01 05.0	+02 52 25	43	42
SMM J02399−0134	11.0	02 39 56.4	−01 34 27	12	12
SMM J22471−0206	9.2	22 47 10.2	−02 05 56	84	32
SMM J02400−0134	7.6	02 39 57.8	−01 34 51	122	74
SMM J04431+0210	7.2	04 43 07.2	+02 10 24	22	74
SMM J21536+1742	6.7	21 53 38.4	+17 42 16	73	59
SMM J00265+1710	6.1	00 26 31.3	+17 10 04	66	60
SMM J22472−0206	6.1	22 47 13.9	−02 06 11	64	102
SMM J00266+1710	5.9	00 26 37.9	+17 09 51	104	...
SMM J00267+1709	5.0	00 26 39.7	+17 09 12	110	...
SMM J04433+0210	4.5	04 43 15.0	+02 10 02	100	...

Notes.—Units of right ascension are hours, minutes, and seconds, and units of declination are degrees, arcminutes, and arcseconds. The positions represent the location of the submillimeter emission, and the sources are listed in decreasing order of 850 μm flux density (Smail et al. 2002). Shorter NIRC integrations were done for the bright sources (e.g., SMM J02399−0136 and SMM J02399−0134), while longer observations were carried out for fainter sources.

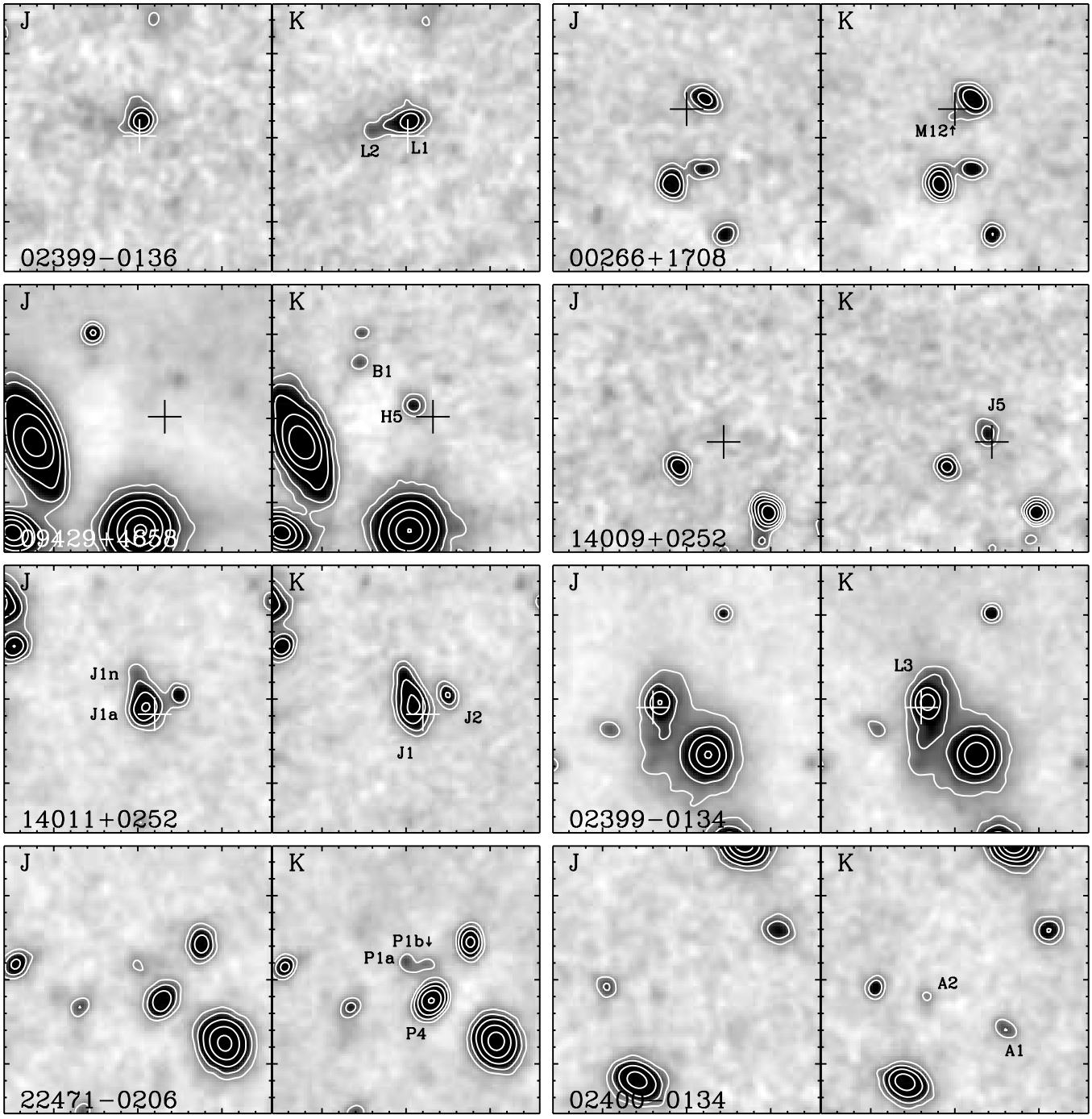

FIG. 1.—NIRC *J*-band (1.2 μm) and *K*-band (2.2 μm) images of the SMG fields (north is up and east is left). The images are $16'' \times 16''$ with tick marks every $1''$. The images are centered on the position of the 850 μm emission given in Table 1. For the confirmed SMG counterparts, plus signs indicate the position of the CO, millimeter, or radio emission. The data have been smoothed with a $0''.5$ FWHM Gaussian. The gray scale is plotted on a logarithmic scale, from $-3\ \sigma$ (*white*) to $+15\ \sigma$ (*black*), and the contours start at $+5\ \sigma$ and increase by factors of 2. The last three fields only have *K*-band data.

stars. Sources with blended components were measured using SExtractor. For the faint SMGs M12 and N4, the bright nearby foreground galaxies were subtracted from the images before aperture measurements were made (e.g., Frayer et al. 2003). For comparison with the known SMGs and to search for possible new counterparts, all sources detected above the $3\ \sigma$ level were measured. The images are about 1–2 mag deeper than the previous *K*-band observations of the fields (Smail et al. 2002), and the photometric results in this paper are consistent with those measured previously.

Figure 2 shows the $J-K$ colors as a function of *K*-band magnitude for the 339 sources detected in the 12 fields with both *J*- and *K*-band imaging. The survey limits for the data are approximately $K < 22.5$ mag and $J < 24.5$ mag ($3\ \sigma$). Typical galaxies in the foreground clusters ($z = 0.2$–0.4) are expected to have colors of $J-K \lesssim 1.6$ mag, while the background galaxies at $z > 1$ are expected to have colors of $J-K > 1.5$ mag (e.g., Totani et al. 2001b). The seven confirmed SMG counterparts in the sample have $J-K$ colors ranging from 1.7 to greater than 4.6 mag. The bright SMGs

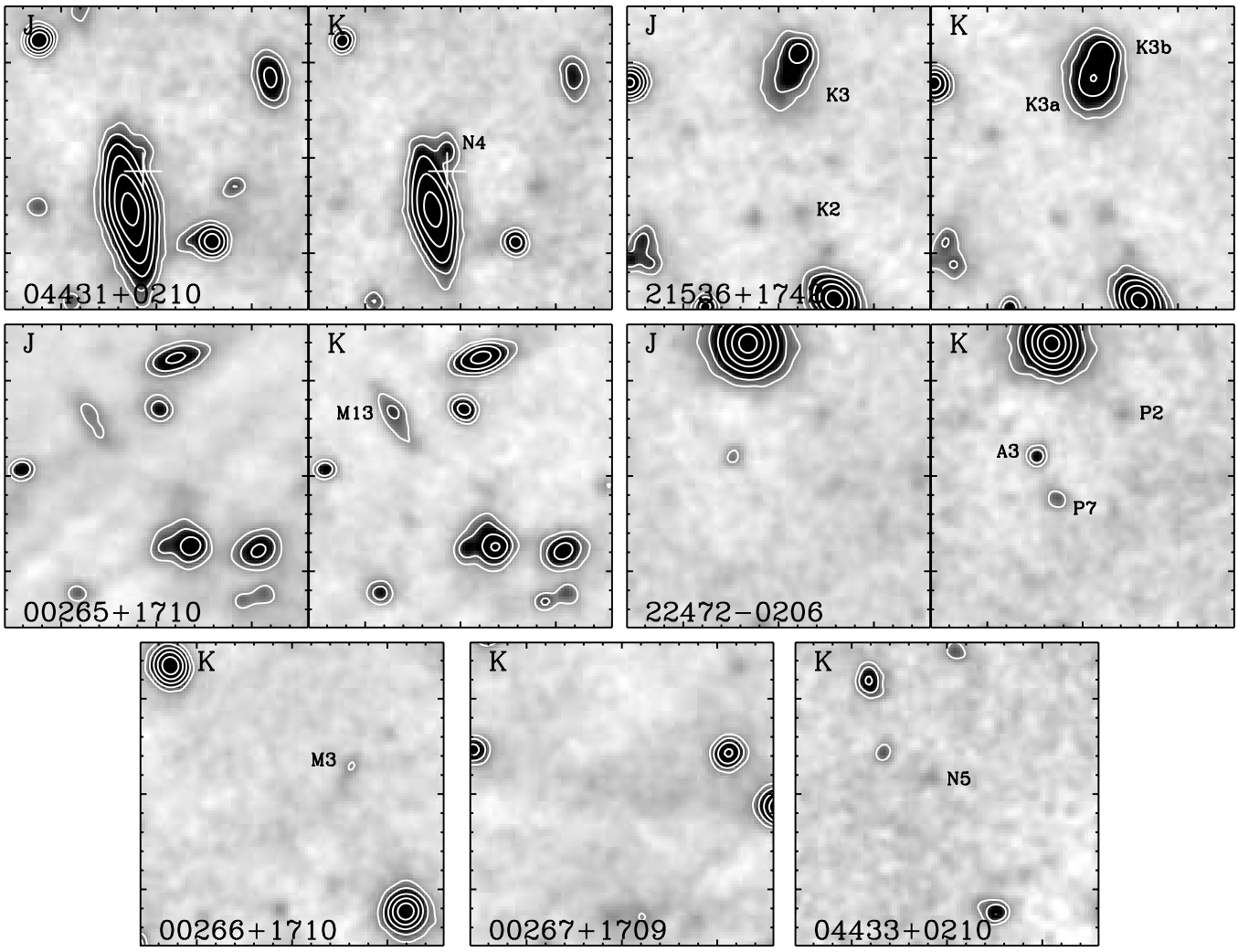

FIG. 1.—*Continued*

($K < 19$ mag) are bluer ($J-K \sim 2$ mag) than the fainter SMGs, which tend to show extremely red NIR colors ($J-K \gtrsim 3$ mag). The NIR results suggest that the $J-K$ colors can be used to help identify candidate SMG counterparts. Based on this sample, bright, relatively blue NIR sources ($K < 19$ mag with $J-K < 1.5$ mag) and the fainter sources ($K > 20$ mag) out to a redder limit of $J-K < 2$ mag are not likely to be the counterparts of typical SMGs.

Besides the confirmed and candidate SMG counterparts, we have uncovered several additional sources in the fields that have very red ($J-K > 2.5$ mag) or extremely red ($J-K > 3$ mag) NIR colors. All of the extremely red sources are faint ($K > 19$ mag), presumably since bright, extremely red sources are rare (e.g., Totani et al. 2001b) and the survey covers a small area. In total, we find 13 sources with $J-K > 2.5$ mag and nine sources with $J-K > 3$ mag. The reddest source in the sample has $J-K > 4.9$ mag (3 σ), which is the reddest galaxy in the NIR known to date. In comparison, the previous reddest galaxy has $J-K > 4.5$ mag and was found in the Hubble Deep Field (Dickinson et al. 2000).

3.2. *Individual Submillimeter Galaxies*

The identification of the counterparts of the SMGs in the SCUBA Cluster Lens Survey has been discussed previously (Smail et al. 2002 and references therein). We now present details of the new candidate counterparts and the additional knowledge gained from the deep NIR imaging of the fields.

SMM J09429+4658.—Smail et al. (1999) identified this source as H5 based on its extremely red $R-K$ color and an accurate radio position. The deep J-band data for H5 indicate an extremely red NIR color of $J-K > 4.57$ mag (3 σ). This is the reddest known NIR counterpart to an SMG. The source B1, which is 4″ northeast of H5, also shows an extremely red NIR color of $J-K > 3.84$ mag. It is not known if this source is associated with H5; neither source has a redshift. However, the likelihood of randomly finding two $J-K \gtrsim 4$ mag sources within 5″ is less than 0.001 (Totani et al. 2001b), which suggests that the two galaxies could be related. Unlike H5, B1 is detected at optical wavelengths and is not an ERO based strictly on its $R-K$ color.

SMM J22471−0206.—P1 has been considered a possible counterpart based on its tadpole morphology (Smail et al. 1998). The relatively blue $J-K < 2$ mag color for P1 is circumstantial evidence against it being the SMG counterpart. Smail et al. (2002) and Barger et al. (1999b) suggest that P4 may be the SMG counterpart based on its morphology, red color, and the presence of an active galactic nucleus (AGN). The argument against P4 is the fact that its high submillimeter-

TABLE 2
PHOTOMETRY MEASUREMENTS

Field	Source	Offset (α, δ) (arcsec)	Aperture Diameter (arcsec)	K (mag)	J (mag)	$J-K$ (mag)	Comments	Ref.
02399−0136	L1	−0.3, 1.0	3	18.09 ± 0.06	20.07 ± 0.08	1.98		
	L2	1.9, 0.5	2	20.29 ± 0.13	22.43 ± 0.15	2.14		
	L1+L2	...	6	17.79 ± 0.07	19.79 ± 0.07	2.00	SMG:CO	1, 2
00266+1708	M12	0.1, 1.2	2	22.36 ± 0.16	>24.27	>1.91	SMG:mm	3
09429+4658	H5	−0.5, 0.7	2	19.73 ± 0.08	>24.20	>4.47	SMG:radio	4
	B1	2.7, 3.3	2	20.48 ± 0.12	>24.32	>3.84		
14009+0252	J5	−1.9, −0.9	2	20.52 ± 0.09	23.87 ± 0.21	3.35	SMG:radio	5
14011+0252	J1	−0.4, −0.4	6	17.71 ± 0.05	19.45 ± 0.05	1.74	SMG:CO	5, 6, 7, 8
	J1a	−0.4, −0.4	3	17.86 ± 0.06	19.62 ± 0.06	1.76		
	J1n	0.2, 1.7	2	19.89 ± 0.13	21.76 ± 0.11	1.87		
	J2	−2.4, 0.4	2	19.76 ± 0.07	21.39 ± 0.07	1.63		
	J1+J2	...	6	17.56 ± 0.05	19.28 ± 0.05	1.72		
02399−0134	L3	1.6, −0.1	6	16.02 ± 0.05	17.84 ± 0.05	1.82	SMG:CO	9, 10
22471−0206	P4	−1.5, −1.2	3	17.53 ± 0.06	19.82 ± 0.06	2.29	SMG?	
	P1a	0.0, 1.1	2	20.41 ± 0.08	22.01 ± 0.08	1.60		
	P1b	−1.2, 0.9	2	21.02 ± 0.10	23.01 ± 0.12	1.99		
02400−0134	A1	−3.0, −2.9	2	20.73 ± 0.08	23.59 ± 0.17	2.86	SMG?	
	A2	1.7, −0.9	2	21.55 ± 0.12	24.09 ± 0.26	2.54		
04433+0210	N4	0.7, 0.4	2	19.41 ± 0.09	22.56 ± 0.28	3.15	SMG:CO	11, 12
21536+1742	K2	−1.2, −3.0	2	21.46 ± 0.16	22.79 ± 0.15	1.33		
	K3	−0.8, 4.7	6	17.23 ± 0.05	19.26 ± 0.05	2.03	SMG?	
	K3a	−0.6, 4.2	3	17.95 ± 0.05	20.25 ± 0.06	2.30		
	K3b	−1.1, 5.5	3	18.41 ± 0.05	20.21 ± 0.06	1.80		
00265+1710	...	0.0, 0.0	2	>22.47	>22.85	...	Nondetection	
	M13	3.5, 3.3	2	19.41 ± 0.07	20.96 ± 0.07	1.55		
22472−0206	P7	1.4, −1.2	2	21.05 ± 0.13	>24.72	>3.67	SMG?	
	P2	−2.1, 3.2	2	21.93 ± 0.25	23.78 ± 0.17	1.85		
	A3	2.4, 1.1	2	20.58 ± 0.09	23.29 ± 0.11	2.71		
00266+1710	...	0.0, 0.0	2	>22.46	...	...	Nondetection	
	M3	−3.2, 1.5	2	21.10 ± 0.11	...	...		
00267+1709	...	0.0, 0.0	2	>21.85	...	...	Nondetection	
04433+0210	N5	0.9, −0.8	2	22.43 ± 0.24	...	...	SMG:radio?	

NOTES.—Offsets are with respect to the submillimeter positions given in Table 1. Lower limits are 3 σ. The candidate SMGs are shown with a question mark. The confirmed SMGs are listed without question marks and are discussed in the references indicated in the last column:

REFERENCES.—(1) Ivison et al. 1998; (2) Frayer et al. 1998; (3) Frayer et al. 2000; (4) Smail et al. 1999; (5) Ivison et al. 2000; (6) Frayer et al. 1999; (7) Ivison et al. 2001; (8) Downes & Solomon 2003; (9) Soucail et al. 1999; (10) J.-P. Kneib 2003, private communication; (11) Frayer et al. 2003; (12) Neri et al. 2003.

to-radio flux density ratio is inconsistent with its low redshift of $z = 1.16$, assuming a standard dust temperature of $T \sim 40$–50 K. If P4 is the submillimeter counterpart, the upper-limit on the 1.4 GHz radio emission implies a dust temperature of less than about 22 K (see Blain, Barnard, & Chapman 2003), even cooler than the two cold dusty galaxies found in the FIRBACK survey (Chapman et al. 2002b). No other new candidate sources were found in this field from the NIR data. P4 is currently the best candidate detected near the submillimeter position given its relatively red color of $J-K = 2.3$ mag, but its identification is not conclusive.

SMM J02400−0134.—Smail et al. (2002) classified this as a blank field, but deep NIR imaging has uncovered two possible counterparts. The redder source A1 ($J-K = 2.9$ mag) is near the position of source 2 of Cowie et al. (2002), while A2, which is nearly as red in the NIR ($J-K = 2.5$ mag), lies closer to the position of Smail et al. (2002). It is possible that the submillimeter emission arises from both sources. Given that the Cowie et al. (2002) SCUBA observations are deeper, we suggest A1 is the most likely candidate SMG for the field.

SMM J21536+1742.—The faint source K2 near the submillimeter position of Smail et al. (2002) has a relatively blue $J-K = 1.3$ mag color and is not believed to be the counterpart. K3 shows a strong NIR color gradient between components K3a ($J-K = 2.3$ mag) and K3b ($J-K = 1.8$ mag). The submillimeter centroid from Cowie et al. (2002) is positionally coincident with that of a weak ISOCAM source (object ID 43; Metcalfe et al. 2003) and is near K3a. The red NIR color of K3a is consistent with the identification of K3 as the SMG counterpart.

SMM J00265+1710.—The source designated M13 (Fig. 1) is possibly associated with radio emission (Smail et al. 2002), but its relatively blue $J-K$ color suggests that it is not likely to be the SMG. This SMG is considered to be a nondetection down to $K > 22.5$ mag (3 σ).

SMM J22472−0206.—Although P2 ($K = 21.9$ mag) is at high-redshift ($z = 2.1$; Barger et al. 1999b), it is not thought to be the SMG based on its blue $J-K < 2$ mag color (Table 2). The reddest source in the field P7 ($J-K > 3.8$ mag) is also nearest to the submillimeter position and is adopted as the likely SMG candidate counterpart. The nearby source A3 (Fig. 1) is very red as well ($J-K = 2.7$ mag) and may be associated with P7.

SMM J04433+0210.—This SMG is the weakest submillimeter source in the survey and is possibly associated with a weak radio detection (Smail et al. 2000) at the position of N5 (Smail et al. 2002). We find a faint K-band magnitude of 22.4 for N5. Since no other sources were detected in the

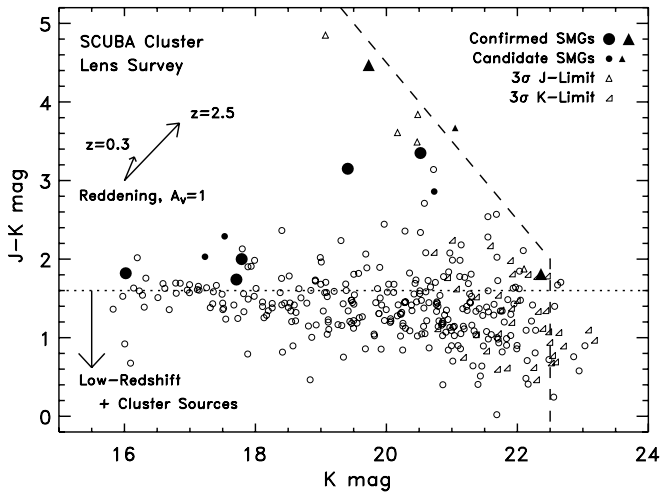

FIG. 2.—Photometry results for all 339 detected sources in the 12 SMG fields with *J*- and *K*-band observations. The confirmed and candidate SMG counterparts are plotted as large and small solid symbols, respectively. Circles represent detections in both the *J*- and *K*-bands, upward pointing triangles show *K*-band detections with 3 σ *J*-band limits, and triangles pointed toward the lower-right show *J*-band detections with 3 σ *K*-band limits. Almost all sources below the dotted line ($J-K < 1.6$ mag) are expected to be low-redshift sources and cluster galaxies. The dashed line represents the survey limits of $K < 22.5$ mag and $J < 24.5$ mag (3 σ). The background SMGs would need to be shifted about 1 mag fainter in *K*-band on average to correct for lensing. Reddening vectors are shown for a source-frame visual extinction of $A_V = 1$ mag at the typical cluster ($z = 0.3$) and SMG ($z = 2.5$) redshifts, assuming the standard Galactic interstellar extinction law (Whitford 1958).

K-band near the submillimeter position that were not already seen in the *I*-band data, N5 remains the best candidate SMG counterpart.

4. DISCUSSION

The current status regarding the counterparts of the 15 SMGs in the SCUBA Cluster Lens Survey can be summarized as follows: Seven SMGs have reliable counterparts (L1/L2, J1, M12, H5, J5, L3, and N4) based on accurate positions from CO, radio, and/or millimeter interferometric continuum observations (Frayer et al. 1998, 1999, 2000; Smail et al. 2000; Ivison et al. 2000; J.-P. Kneib et al. 2003, private communication; R. Neri et al. 2003). An additional five SMGs have candidate counterparts (§ 3.2): P4 for SMM J22471−0206, A1 for SMM J02400−0134, K3 for SMM J21536+1708, P7 for SMM J22472−0206, and N5 for SMM J04433+0210. The three remaining fields (SMM J00265+1710, SMM J00266+1710, and SMM J0267+1709) are still considered undetected to about $K \gtrsim 23$ (3 σ), after correcting for lensing. The faintest submillimeter sources in the survey may be affected by confusion and/or may even represent spurious 850 μm detections in some cases. The limitations due to confusion have been previously discussed (e.g., Eales et al. 2000; Blain et al. 2002). Seven of the nine brightest SMGs (Table 1) detected above 4 σ at 850 μm (Smail et al. 2002) have confirmed counterparts, and all nine of the brightest SMGs have candidate NIR counterparts.

4.1. *Near-Infrared Properties of Submillimeter Galaxies*

Figure 2 shows that SMGs tend to be either relatively bright ($K \lesssim 19$ mag) with normal NIR colors consistent with high redshifts ($z > 1$) or faint with extremely red colors ($J-K \gtrsim 3$ mag). The distinct color difference between the bright SMGs and the faint extremely red SMGs is consistent with about 3 mag of additional source-frame visual extinction for the fainter sources, assuming typical SMG redshifts of $z \sim 2$–3. However, since the SMGs do not appear uniformly distributed along the reddening vector (Fig. 2), reddening may not be the only explanation for the variation of the NIR colors. A dichotomy of colors for SMGs has previously been seen in $I-K$ (e.g., Smail et al. 2002) and has been used as a classification scheme in which the Class I SMGs are relatively bright sources and the Class II sources are faint and extremely red (Ivison et al. 2000). The NIR data are consistent with the presence of two classes of SMGs based on colors. There are many possible origins that could contribute to the variations of colors including reddening, the presence of an AGN, the presence of unobscured companions, and/or different evolved stellar masses.

With several undetected SMGs, the average *K*-band magnitude is still indeterminate, but we can estimate the median *K*-band magnitude for the SMG population. We correct for lensing by using the amplification factors given by Smail et al. (2002) and Cowie et al. (2002). For sources without known amplification factors, we adopt an average value of 2.5. Assuming all of the candidate SMG counterparts are correct, the median *K*-band magnitude is $K = 21.0$ mag. This result is likely biased by the selection effect that it is easier to detect brighter candidates and should probably be considered as a lower bound. An upper bound of $K < 23.3$ mag can be estimated by assuming all of the candidate counterparts with $J-K < 3$ mag are actually still undetected. The median magnitude of the SMG population is thus likely to be $K = 22 \pm 1$ mag.

At the average redshift of about $z \sim 2.5$ for a significant fraction of the SMG population (Chapman et al. 2003b), the observed *K*-band emission represents rest-frame optical *R*-band light. By comparing the observed NIR properties of SMGs with the optical properties of ultraluminous infrared galaxies (ULIRGs; $L_{\rm ir} > 10^{12}\ L_\odot$), we can test the hypothesis that SMGs are analogous to the low-redshift population of ULIRGs. The median $K = 22$ mag for the SMG population corresponds to an absolute magnitude of $M_R = -21.5$ mag at $z = 2.5$. For the low-redshift *IRAS* 1 Jy ULIRG sample, the median *R*-band absolute magnitude is $M_R = -21.9$ mag, corresponding to $2L^*$ (Kim, Veilleux, & Sanders 2002). Therefore, SMGs have comparable optical luminosities to local ULIRGs and thus likely represent massive systems.

The median NIR color of the six confirmed SMG counterparts with meaningful NIR colors is $J-K = 2.6 \pm 0.6$ mag. Including the additional candidate counterparts does not change the median value. However, given the selection effect that brighter sources that tend to have bluer NIR colors are easier to detect, the true median $J-K$ color of the SMG population may be significantly redder. We can compare the observed $J-K$ colors with the corresponding rest-frame $U-R$ colors found for ULIRGs. We calculate a median color of $U-R = 1.15$ mag for the sample of ULIRGs with global *U*-band measurements from Surace & Sanders (2000) and global *R*-band measurements from Kim et al. (2002). At a redshift of $z = 2.5$, the median $U-R$ color of local ULIRGs would correspond to an NIR color of $J-K = 2.7$ mag, in close agreement with the SMGs. Low-redshift ULIRGs show a broad range of colors, presumably due to patchy extinction. From the full range of $U-R$ colors found for ULIRGs, we could expect colors of $J-K = 1$–4.2 mag for the SMGs. We have yet to identify any SMGs with colors as blue as the

bluest ULIRGs, but we have detected SMGs redder than the reddest known ULIRGs (e.g., H5).

In comparison, the Lyman break population of galaxies, which have similar redshifts to those of the SMG population, are significantly bluer, with an average value of $J-K_s = 1.5$ mag (Shapley et al. 2001). Therefore, in terms of rest-frame optical colors, SMGs are more similar to low-redshift ULIRGs than to typical Lyman break galaxies.

Most SMG counterparts are not compact. We fitted an elliptical Gaussian to the *K*-band data to measure the FWHM of the core of the SMG counterparts. After deconvolution with the stellar point-spread function, the central FWHM of the SMG cores ranges in size from less than 0.″5 to 2.″1. The median core size is 1.″3 for the seven confirmed SMGs and is 1.″2 including the candidate counterparts. Assuming typical SMG redshifts of $z = 2$–3 (Smail et al. 2002; Chapman et al. 2003b), the radius of the SMG cores is about 2 kpc, corrected for lensing. The sizes of the SMGs are similar to those derived for the bright central regions of ULIRGs (Surace et al. 1998; Scoville et al. 2000) and are comparable to the bulge sizes found for normal galaxies. These results are consistent with the scenario that the SMGs represent the formative phases of the bulges of galaxies or the cores of massive elliptical galaxies (Lilly et al. 1999).

Several SMG counterparts show multiple components suggesting that mergers play a significant role for the SMG population. Nearly all local ULIRGs have been shown to arise from mergers based on optical morphologies that show strongly interacting pairs with apparent tidal tails and distorted galaxies with close double nuclei (Murphy et al. 1996; Surace et al. 1998). The unusual optical morphologies are a distinguishing characteristic of ULIRGs. Unfortunately, the NIR data for the SMGs lack both the surface brightness sensitivity required to detect tidal features and the resolution required to resolve close pairs (<5 kpc), making detailed morphological comparisons between ULIRGs and SMGs impractical with the current data. For the 1 Jy ULIRG survey, 28% of ULIRGs show nuclear separations of more than 5 kpc (Veilleux, Kim, & Sanders 2002). In comparison, 2/7 (29%) of the confirmed SMGs and 3/12 (25%) of the confirmed plus candidate SMGs show double components with similarly large separations.

The measured rest-frame optical properties of the SMGs are consistent with those of low-redshift ULIRGs. Previously the SMGs have been shown to have infrared, CO, and radio properties similar to those of ULIRGs (e.g., Frayer et al. 1998, 1999; Ivison et al. 2000). The NIR data suggest that SMGs also have similar rest-frame optical properties. The optical luminosities, sizes, and morphologies of SMGs are consistent with massive ($\gtrsim M^*$) galaxies and major merger events and not high-redshift subgalactic clumps (e.g., Pascarelle et al. 1996).

4.2. *Extremely Red J−K Galaxies*

Accounting for lensing (average amplification of 1 mag), this survey reached depths of approximately $K = 23.5$ and $J = 25.5$ mag, which is as deep as the deepest previous NIR surveys (Maihara et al. 2001; Franx et al. 2003). We observed 10 fields in both *J* and *K* band to interesting depths, covering 4.4 arcmin^2 on the sky. Correcting for lensing, the source-plane area surveyed is only about 1.8 arcmin^2. We detected nine sources with $J-K > 3$ mag, yielding a source density of 5 arcmin^{-2} at $K < 22.5$ mag ($J < 25.5$ mag). In comparison, the number density of $J-K > 3$ mag sources to similar depths is about 1 arcmin^{-2} from the blank-field surveys (Totani et al. 2001a, 2001b; Franx et al. 2003). Given that SMGs tend to show extremely red colors, it is not surprising to find a high number of $J-K > 3$ mag sources in observations targeted at the positions of SMGs. If we ignore all the $J-K > 3$ mag SMG candidate counterparts and potential companions within 10″, the number density of extremely red NIR sources decreases to about 2 arcmin^{-2} in the SMG fields. Although roughly consistent with the blank-field result within the errors associated with small number statistics, the slight excess may indicate an enhanced density of ERO neighbors for the SMG population, as recently suggested by Takata et al. (2003).

At a source density of 2 arcmin^{-2}, the probability of randomly finding a $J-K > 3$ mag source on the sky within the 15″ SCUBA beam is more than 10%. Therefore, the chance of finding an extremely red source associated with a SCUBA detection is not negligible. For the strongest SCUBA detections ($\gtrsim 5\ \sigma$), the 850 μm centroid positions are known to within about $\pm 3''$, which decreases the probability of a chance positional coincidence to less than 1%. We argue as a result that candidate sources with $J-K \gtrsim 3$ mag within 5″ of the 850 μm position indicate likely counterparts, but that a red $J-K$ color by itself is not sufficient to confirm an SMG counterpart.

The fraction of very and extremely red sources that are SMGs may increase with redder colors. Of the 13 sources in the fields with $J-K > 2.5$ mag, only five are candidate SMG counterparts, while four out of the nine of the $J-K > 3$ mag sources are suspected SMGs (H5, J5, N4, and P7). One of the $J-K > 3$ mag sources is arguably a companion to H5 (B1, § 3.2). The relationship of the remaining four $J-K > 3$ mag sources to the SMG population is not clear. As discussed by Totani et al. (2001b), the density of SMGs is similar to that of extremely red NIR sources, suggesting a possible connection between dusty SMGs and galaxies with extremely red colors. It is possible that the remaining four $J-K > 3$ mag galaxies are simply SMGs below the 2 mJy 850 μm sensitivity limit of the SCUBA Cluster Lens Survey (corrected for lensing). At the fainter limit of 1 mJy the number density of SMGs (Blain et al. 2002) is sufficient to account for the number of extremely red sources.

Based on this survey, SMGs with $J-K > 3$ mag account for greater than 40% of the integrated 850 μm background flux above 5 mJy, correcting for lensing. Although many SMGs have extremely red $J-K$ colors, it is not clear whether most $J-K > 3$ mag sources are infrared-bright SMGs. Nearly all of the confirmed SMGs to date have extremely high luminosities ($L \sim 10^{13}\ L_\odot$). If the majority of the $J-K > 3$ mag sources are examples of less luminous SMGs ($L \lesssim 10^{12}\ L_\odot$), then their high counts would imply that this population may be responsible for a large fraction of the star formation activity at high redshift. Alternatively, the majority of the faint $J-K > 3$ mag sources may have much lower luminosities; it has even been proposed that many may be Lyman break galaxies at $z \gtrsim 10$ (e.g., Dickinson et al. 2000; Im et al. 2002). Observations with the *Space Infrared Telescope Facility* (*SIRTF*) will help to distinguish between $z \gtrsim 10$ Lyman break systems and dust-reddened moderate redshift systems from their spectral energy distributions.

5. CONCLUSIONS

Using deep NIR images of the SMGs in the SCUBA Cluster Lens Survey, we find that a color selection criterion of

$J-K \gtrsim 3$ mag can be used to help identify candidate counterparts of SMGs that are too faint to be detected at optical and radio wavelengths. Faint sources ($K > 20$ mag) with $J-K < 2$ mag can probably be ruled out as SMG counterparts.

Of the 15 sources in the survey, all six of the brightest submillimeter sources with intrinsic 850 μm fluxes of $\gtrsim 5$ mJy are identified at 1.4 GHz and are moderately or very red in $J-K$. The remaining nine fainter sources lack strong radio detections, but we identify likely counterparts for over half of these SMGs, based in part on their extreme $J-K$ colors. Only 3/15 of the sources in the survey remain unidentified ($K >$ 23 mag, corrected for lensing), all of which are faint at submillimeter wavelengths. These may be either more distant and/or more obscured SMGs, or simply highly confused or spurious sources at 850 μm.

The data on the SMG fields confirm the conclusion from blank-field surveys that the fraction of extremely red NIR sources increases dramatically at fainter magnitudes. Within the SMG fields, we find a number density of 5 arcmin^{-2} for sources with $J-K > 3$ mag ($K < 22.5$ mag), which is significantly higher than the number density of bright SMGs. It is not clear if the excess of extremely red NIR sources represents weaker infrared-luminous galaxies with $S(850\ \mu\text{m}) \lesssim 2$ mJy, which are undetected by SCUBA, or if they represent a different population of sources.

The median K-band magnitude for the SMG population is $K = 22 \pm 1$ mag, and their median color is $J - K = 2.6 \pm 0.6$ mag. Future observations with the *SIRTF* and the Atacama Large Millimeter Array will confirm or refute candidate counterparts. The colors, rest-frame optical luminosities, sizes, and morphologies are all consistent with the properties of low-redshift ULIRGs and the association of SMGs with merger activity that may lead to the formation of elliptical galaxies or the bulges of galaxies.

We thank the staff at the Keck Observatory who have made these observations possible. We are most fortunate to have the opportunity to conduct observations from the summit of Mauna Kea, which has a very significant cultural role within the indigenous Hawaiian community. We acknowledge J. Surace, R. Ivison, J.-P. Knieb, L. Yan, and M. Im for discussions about ULIRGs, SMGs, and EROs. We thank D. Thompson for his NIRCtools data reduction package and C. Frayer for proofreading the manuscript. D. T. F. and L. A. are supported by the Jet Propulsion Laboratory, California Institute of Technology, under contract with NASA. A. W. B., N. A. R., and I. R. S. acknowledge support from the NSF grant AST 02-05937, an NSF Graduate Research Fellowship, and both the Royal Society and the Leverhulme Trust, respectively.

REFERENCES

Barger, A. J., Cowie, L. L., Richards, E. A. 2000, AJ, 119, 2092
Barger, A. J., Cowie, L. L., & Sanders, D. B. 1999a, ApJ, 518, L5
Barger, A. J., Cowie, L. L., Smail, I., Ivison, R. J., Blain, A. W., & Kneib, J.-P. 1999b, AJ, 117, 2656
Bertin E., & Arnouts S., 1996, A&AS, 117, 393
Blain, A. W., Barnard, V. E., & Chapman, S. C. 2003, MNRAS, 338, 733
Blain, A. W., Smail, I., Ivison, R. J., Kneib, J.-P., & Frayer, D. T. 2002, Phys. Rep., 369, 111
Chapman, S. C., et al. 2003a, ApJ, 585, 57
Chapman, S. C., Blain, A. W., Ivison, R. J., & Smail, I. R. 2003b, Nature, 422, 695
Chapman, S. C., Richards, E. A., Lewis, G. F., Wilson, G., & Barger, A. J. 2001, ApJ, 548, L147
Chapman, S. C., Scott, D., Borys, C., & Fahlman, G. G. 2002a, MNRAS, 330, 92
Chapman, S. C., Smail, I., Ivison, R. J., Helou, G., Dale, D. A., & Lagache, G. 2002b, ApJ, 573, 66
Cowie, L. L., Barger, A. J., & Kneib, J.-P. 2002, AJ, 123, 2197
Dickinson, M., et al. 2000, ApJ, 531, 624
Downes, D., & Solomon, P. M. 2003, ApJ, 582, 37
Eales, S., Lilly, S., Gear, W., Dunne, L., Bond, J. R., Hammer, F., Le Fèvre, O., & Crampton, D. 1999, ApJ, 515, 518
Eales, S., Lilly, S., Webb, T., Dunne, L., Gear, W., Clements, D., & Yun, M. 2000, AJ, 120, 2244
Franx, M., et al. 2003, ApJ, 587, L79
Frayer, D. T., Armus, L., Scoville, N. Z., Blain, A. W., Reddy, N. A., Ivison, R. J., & Smail, I. 2003, AJ, 126, 73
Frayer, D. T., et al. 1999, ApJ, 514, L13
Frayer, D. T., Ivison, R. J., Scoville, N. Z., Yun, M., Evans, A. S., Smail, I., Blain, A. W., & Kneib, J.-P. 1998, ApJ, 506, L7
Frayer, D. T., Smail, I., Ivison, R., J., & Scoville, N. Z. 2000, AJ, 120, 1668
Hughes, D., et al. 1998, Nature, 394, 241
Im, M., Yamada, T., Tanaka, I., & Kajisawa, M. 2002, ApJ, 578, L19
Ivison, R. J., et al. 2002, MNRAS, 337, 1
Ivison, R. J., Smail, I., Barger, A. J., Kneib, J.-P., Blain, A. W., Owen, F. N., Kerr, T. H., & Cowie, L. L. 2000, MNRAS, 315, 209
Ivison, R. J., Smail, I., Frayer, D. T., Kneib, J.-P., & Blain, A. W. 2001, ApJ, 561, L45
Ivison, R. J., Smail, I., Le Borgne, J.-F., Blain, A. W., Kneib, J.-P., Bézecourt, J., Kerr, T. H., & Davies, J. K. 1998, MNRAS, 298, 583
Kim, D.-C., Veilleux, S., & Sanders, D. B. 2002, ApJS, 143, 277
Lilly, S. J., Eales, S. A., Gear, W. K. P., Hammer, F., Le Fèvre, O., Crampton, D., Bond, J. R., & Dunne, L. 1999, ApJ, 518, 641
Maihara, T., et al. 2001, PASJ, 53, 25
Matthews, K., & Soifer, B. T. 1994, Infrared Astronomy with Arrays: The Next Generation, ed. I. McLean (Dordrecht: Kluwer), 239
Metcalfe, L., et al. 2003, A&A, 407, 791
Murphy, T. W., Jr., Armus, L., Matthews, K., Soifer, B. T., Mazzarella, J. M., Shupe, D. L., Strauss, M. A., & Neugebauer, G. 1996, AJ, 111, 1025
Neri, R., et al. 2003, ApJ, 597, L113
Pascarelle, S. M., Windhorst, R. A., Keel, W. C., & Odewahn, S. C. 1996, Nature, 383, 45
Persson, S. E., Murphy, D. C., Krzeminski, W., Roth, M., & Rieke, M. J. 1998, AJ, 116, 2475
Scott, S. E., et al. 2002, MNRAS, 331, 817
Scoville, N. Z., et al. 2000, AJ, 119, 991
Shapley, A. E., Steidel, C. C., Adelberger, K. L., Dickinson, M., Giavalisco, M., & Pettini, M. 2001, ApJ, 562, 95
Smail, I., Ivison, R. J., & Blain, A. W. 1997, ApJ, 490, L5
Smail, I., Ivison, R. J., Blain, A. W., & Kneib, J.-P. 1998, ApJ, 507, L21
———. 2002, MNRAS, 331, 495
Smail, I., Ivison, R. J., Kneib, J.-P., Cowie, L. L., Blain, A. W., Barger, A. J., Owen, F. N., & Morrison, G. 1999, MNRAS, 308, 1061
Smail, I., Ivison, R. J., Owen, F. N., Blain, A. W., & Kneib, J.-P. 2000, ApJ, 528, 612
Soucail, G., Kneib, J. P., Bézecourt, J., Metcalfe, L., Altieri, B., & Le Borgne, J. F. 1999, A&A, 343, L70
Surace, J. A., & Sanders, D. B. 2000, AJ, 120, 604
Surace, J. A., Sanders, D. B., Vacca, W. D., Veilleux, S., & Mazzarella, J. M. 1998, ApJ, 492, 116
Takata, T., et al. 2003, PASJ, 55, 789
Totani, T., Yoshii, Y., Iwamuro, F., Maihara, T., & Motohara, K. 2001a, ApJ, 559, 592
Totani, T., Yoshii, Y., Maihara, T., Iwamuro, F., & Motohara, K. 2001b, ApJ, 558, L87
Veilleux, S., Kim, D.-C., & Sanders, D. B. 2002, ApJS, 143, 315
Webb, T. M., et al. 2003, ApJ, 587, 41
Wehner, E. H., Barger, A. J., & Kneib, J.-P. 2002, ApJ, 577, L83
Whitford, A. E. 1958, AJ, 63, 201